Curvature Tuned Preparation of nano-liposomes

Rükan Genç[1], Mayreli Ortiz[1,], Ciara K. O'Sullivan[1,2,*]*

[1]Nanobiotechnology and Bioanalysis Group, Department of Chemical Engineering, Universitat Rovira I Virgili, Av. Països Catalans, 26, 43007, Tarragona, Spain.

[2]Institució Catalana de Recerca i Estudis Avançats, Passeig Lluís Companys 23, 08010, Barcelona, Spain.

AUTHOR EMAIL ADDRESS: mayreli.ortiz@fundacio.urv.cat, ciara.osullivan@urv.cat

TITLE RUNNING HEAD: Curvature Tuned Preparation of nano-liposomes

CORRESPONDING AUTHOR FOOTNOTE:

Corresponding authors: telephone: +34-977-558740/8722, Fax: +34-977-559621/8205, E-mail: ciara.osullivan@urv.cat

Corresponding authors: telephone: +34-977-558555/8722, Fax: +34-977-559621/8205, E-mail: mayreli.ortiz@fundacio.urv.cat

ABSTRACT

Numerous methods have been reported for the preparation of liposomes, many of which, in addition to requiring time consuming preparative steps and the use of organic solvents, result in heterogeneous liposome populations of incontrollable size. Taking into consideration the phenomenon of spontaneous vesiculation and the theory of curvature, here we present an extremely rapid and simple, solvent-free

method for the preparation of monodisperse solutions of highly stable small unilamellar vesicles using both charged and zwitterionic lipids mixed with lyso-palmitoylphosphatidylcholine, exploiting a combination of a rapid pH change followed by a defined period of equilibration. Various experimental parameters and their interactions were evaluated in terms of their effect on resulting liposome size and shape, as well as on liposome stability and size distribution, with transmission electron microscope (TEM) imaging being used to visualize the formed liposomes, and Photon correlation spectroscopy to obtain statistical data on mean diameter and monodispersity of the liposome population. Zeta-Potential measurements also provided information on the interpretation of vesiculation kinetics and liposome stability. The time interval of pH jump, operation temperature, equilibration time, as well as lipid type were demonstrated as the determining factors controlling the size, shape and monodispersity of the liposomes. Buffer type was also found to be important for the long-term storage of the liposomes. Ongoing work is looking at the application of the developed method for encapsulation of bioactive molecules, such as drugs, genetic materials and enzymes.

KEYWORDS: liposomes, nano-liposomes, SUVs, preparation method, pH jump

1 INTRODUCTION

The self assembly of building blocks into nano- or micro-structures is an area of intense interest, with lipids being particularly attractive in the formation of closed spherical lipid bilayers known as liposomes.[1,2] Due to the amphiphilic nature of the lipids, liposomes have the capacity to encapsulate a huge number of water-soluble substances in their aquatic core, as well as oil-soluble substances among the lipid bilayer.[3,4] Furthermore, being a natural product, liposomes are of enormous interest as a carrier and encapsulation material in several research areas such as pharmaceuticals,[5] cosmetics,[6] and biosensor technologies,[7,8] and as a model system in cell biology (cell membrane physiology, function and cell-trafficking).[4]

Liposomes can be classified according to their lamellarity- multilamellar (MLV) or unilamellar (UV)-, and size, being defined as small unilamellar vesicles (SUVs) < 100 nm , large unilamellar vesicles (LUVs) 100 nm - 1 μm or giant vesicles > 1 μm.[1] There is a wealth of literature detailing the specific applications of liposomes taking into consideration their size/ structures, and the reader is directed to very recent comprehensive reviews that summarize several advantages of SUVs over larger liposomes regarding their implementation.[3-5,9-13] Examples of these advantages include size-selective cellular-uptake through tumor cells (cancer diagnosis and treatment)[10,13] and from narrow skin capillaries (transdermal drug delivery and cosmetics)[2,14] as well as their size and charge dependent accumulation at brain, spleen, bone marrow, and lung cells (topically or targeted delivery of drugs)[5,15] and higher transfection capacity after cellular-uptake (gene therapy).[9,12] Moreover, they are less recognizable by macrophages, increasing their half-life in the blood stream.[4]

Numerous methods have been described for liposome synthesis.[2] The so-called thin-film preparation method, first described by Bangham in 1965, [16] is the method most used for the preparation of MLVs, and is based on the preparation of a thin-film of lipids, dissolved in organic solvent, (e.g. chloroform/methanol) on the surface of a round bottom flask via rotary evaporation under vacuum, followed by rehydration of the film in an aqueous media containing the substance to be encapsulated.[2,5] The monodispersity of the resulting liposomes depends on the quality of the thin-film, hydration time and agitation conditions. Once MLVs are obtained, additional steps, such as detergent depletion, reverse phase evaporation, sonication or high pressure extrusion, are required to prepare LUVs and SUVs.[2,6] Although sonication is an easy way to prepare SUVs, irreproducibility due to incontrollable process conditions as well as low encapsulation efficiency and stability of the vesicles formed, and potential damage of encapsulated material (DNA, enzyme) caused by the high energy input are major limitations of the method.[6,17] On the other hand, the method of high pressure extrusion has the advantage of producing homogenously sized SUVs of controllable dimension but is not an easy method to scale-up.[6] The “pH jumping method”, first reported by Hauser et al. in 1982, is a relatively fast method for the preparation of

nano-liposomes.[22] The method is based on a rapid change of pH which breaks down MLVs into the SUVs (LUVs and MLVs require subsequent separation using gel chromatography or centrifuge).[20-24] Recently, other research groups have adopted and reported improved versions of the method [24,25]; there is, however, still a requirement for the step of thin-film formation, thus lengthening the preparation time and necessitating the use of organic solvents. Moreover, little attention has been paid to improving the homogeneity of the produced liposomes in size. Mozaffari *et al.* [26,28] and Otake *et al.* [29] reported on the possibility of liposome formation from a non-homogeneous mixture of phospholipids swollen in aqueous solution, demonstrating the possibility to force the lipids to curve into a liposome, without any pre-treatment with organic solvent or use of any additional size homogenization steps, but simply by tuning the curvature of the lipid bilayer under the optimal conditions. There is a growing amount of literature [5,30-36] detailing the curvature theory and the phenomenon of spontaneous vesiculation, which highlight the essential parameters for forcing lipid bilayers to curl into liposomes (i.e, operation temperature, pH, and physicochemical properties of the phospholipids).

Although there are many methods for liposome preparation, fully-defined systems that can provide monodispersed liposome populations of high stability are still required. Taking into account the dynamics of curvature theory, in this study we report on a rapid one-step, solvent-free, method of liposome preparation using a rapid change in pH, ("pH jump"), as one of the driving forces. Several operation parameters and lipid types were studied to probe the effect of each possible factor on the aggregate shape and size. Extremely stable nano-liposomes of highly homogeneous in size were successfully obtained using both charged (negative/positive) and zwitterionic phospholipids of different melting temperatures (T_M). Size distribution and shape of the resulted liposomes were evaluated using both transmission electron microscope (TEM) imaging and photon correlation spectroscopy measurements. Liposome stability was reported as a function of changes in mean diameter and distribution of it, and was confirmed by Z-potential value, which is an indication of the strength of the repulsive interactions between liposomes, which prevent particle flocculation or aggregation.[37] Hence, each variable and its relationship

with other factors is discussed in relation to the Curvature Theory in order to provide a clear understanding of the underlying physical phenomena of the reported method.

2 MATERIALS AND METHODS

2.1 Materials

1,2-Dioleoyl-sn-Glycero-3-[Phospho-rac-(1-glycerol)] (sodium salt) (DOPG), 1,2-Dioleoyl-3-Trimethylammonium-Propane (chloride salt) (DOTAP), 1,2-Dipalmitoyl-sn-Glycero-3-[Phospho-rac-(1-glycerol)] (sodium salt) (DPPG), 1,2-Dioleoyl-sn-Glycero-3-Phosphocholine (DOPC), 1,2-Dipalmitoyl-sn-Glycero-3-Phosphocholine (DPPC) and lyso-palmitoylphosphatidylcholine (lyso-PPC) were supplied as a powder by Avanti Polar Lipids, Inc. and used without further purification. Sodium hydroxide, Hydrochloric acid, di-sodium hydrogen phosphate (anhydrous, reagent grade), Na_2HPO_4), sodium dihydrogen phosphate (anhydrous), extra pure, (NaH_2PO_4) and glycerol 99.5%, reagent grade, were purchased from Scharlau Chemie SA. Sodium chloride was provided by Riedel-de Haën, and MES and HEPES were obtained from Sigma. Milli-Q water (18.2 MΩ.cm) used to prepare buffers and liposomes was obtained using a Simplicity 185 Millipore-Water System.

2.2 Liposome preparation

As an alternative to the thin film preparation step, lipid mixture (50 mg) was directly hydrated in 4 mL buffer (Milli-Q water or 0.01 M, 0.05 M and 0.1 M of MES, HEPES and PBS solutions, respectively) which had previously been heated to a pre-determined temperature, T_o. The temperature was kept constant by placing a glass flask (15 mL) in a water-jacket connected to an UltraTerm 200 Model (P-Selecta) Thermocycler. The mixture was vortexed in a 10 mL falcon tube (with glass beads) for 1-3 min and added to 6 mL of the buffer solution (pH 7.4) (3 % glycerol v/v total). Glycerol was added due to its anti-oxidative properties - via interaction with the polar head group of the lipid, which is useful for long-term

storage of the liposomes.[38] The mixture was left to stir for around 15 min whilst the temperature was kept constant at T_o. The pH was then subsequently raised to a maxima (~ pH 11) using NaOH, and adjusted back to pH 7.4 using HCl for a fixed time period, which we termed as "pH jumping time", Δ**jt**. The resulting mixture was left to mix for a fixed time period of equilibration, Δ**eq**, under the same conditions. Finally, the stirring and heating was stopped and the solution was left to cool to room temperature for 25 min, and subsequently the liposome solution was centrifuged at 1500 rpm for 15 min in order to eliminate possible aggregations and larger sized liposomes, and stored at 4 ºC. All steps were carried out under argon. Until otherwise described, all liposome formulations were phospholipid: lyso-PPC (88:12 mol/mol) which is a typical formulation for the well known temperature sensitive liposomes where Lyso-PPC is used due to its' temperature dependent inducer role in the flexibility and permeability of the liposome membrane.[39] The final lipid mass concentration was kept constant for all lipid formulations at 0.5 % w/v.

2.3 Visualisation of liposome size and shape using Transmission electron microscopy (TEM)

The prepared liposome dispersion was diluted at least three times with buffer. Using a glass pipette, a drop of sample was added to 200-mesh copper grid with a thin film of formvar polymer and left at room temperature until a dried film was obtained. TEM analyses were performed using a Transmission Electron Microscope JEOL 1011 operated at 80 keV with an ultra-high-resolution pole piece providing a point resolution of 2 Å. Micrographs 1024 pixels × 1024 pixels in size were acquired using a Megaview III multiscan-CCD camera. Images were analyzed by iTEM image analysis platform by measuring the diameter of over 100 particles from the photos captured from different parts of the grid and calculating the mean diameter from the data of experiments ($n \geq 3$) carried out using the same parameters obtained from the program.

2.4 Size and size distribution studies using Photon correlation spectroscopy (PCS)

The mean diameter of the liposome emulsions and the size distribution, presented as a function of polydispersity index (PI), were measured using Zeta Sizer 3000H (laser He−Ne (633 nm), detector angle 90°) equipment from Malvern Instruments, Inc., which measures the rate of fluctuation of the light scattered from the particles using photon correlation spectroscopy (PCS). Standard deviations were calculated from the mean of the data of a series of experiments ($n \geq 3$) carried out using the same parameters.

2.5 Z-Potential measurements

Zeta potential measurements were used to characterize changes in the surface charge of lipid aggregates in order to see the relationship between surface charge and stability. Zeta potential values were measured using a Zeta Sizer 3000H (Malvern Instruments, Inc.). Presented standard deviations were calculated from the mean of Z-Pot values of a series of experiments ($n \geq 3$) carried out using the same parameters.

3 RESULTS AND DISCUSSION

3.1 Elucidation of optimum parameters

Lipids spontaneously form aggregates of different shapes depending on their geometry and chemical properties, as well as physical conditions (e.g. temperature, pH and salinity). In addition to these properties, attractive-repulsive forces (Derjaguin, Landau, Verwey and Overbeek (DLVO) Theory) and thermodynamic interactions, due to the amphiphilic and ionic properties of the lipids, have an influence on spontaneous vesiculation.

Two important terms related to the formation of vesicles from lipids are the critical packing parameter, P, and the radius of intrinsic curvature, R_o.

The value of the critical packing parameter, P, is a fundamental term used to explain the packing geometry of the lipid molecule and can be defined by

$$P = V / l \, . \, a \qquad \text{(Eq.1)}$$

where; P is the critical packing parameter, V is molecular volume of surfactant chain, a is area per surfactant head and l is the length of surfactant chain. P should have a value of 0.5-1 to obtain a truncated cone shape lipid, which is the most suitable shape for the lipid to curl into vesicles (Figure 1).[5] During the spontaneous vesiculation process, changes in amphiphile geometry raises the value of P, lowering the curvature (see Eq.1). The effective shape of the molecule can be tuned by changing lipid properties, such as the effective size of the head group, the charge of ionic head group, and changing degree of hydration or, alternatively, can be temperature tuned.[30]

Another important factor, the radius of intrinsic curvature, R_o, defined in eq.2 is the radius of the curvature (see also ref. 35) that minimizes the elastic energy. It does not vary significantly with the lipid geometry but is influenced by factors affecting the lipid tail, such as temperature and degree of unsaturation. It also increases with properties that lead to an increase in the effective head group area (e.g., charge of the head group).

$$\mu e = k \, (1/R - 1/Ro)^2 \qquad \text{(Eq.2)}$$

where; μe is elastic energy, k is elastic constant, R is the radius of curvature/water interface, and R_o is the intrinsic radius of the curvature.[30,35]

Finally, the phase behavior of the lipid has a significant effect on the bilayer curvature. Each phospholipid has a specific main phase transition temperature (T_M) which determines the phase behaviour of the lipids. Above this temperature, the lipid is in a liquid crystalline phase (L_∞), and is fluid; below its T_M, it is in a gel phase and is rigid. Low temperature induces the solid compressed or crystalline phases where the fatty acid tails of the lipids are packed together in a regular arrangement, and thus the limiting

area per molecule is decreased. As the temperature rises, the lipid bilayer changes state from a solid state to a liquid state where the fatty acid tails are more flexible. [2, 16, 30] In the L_∞, R is ∞, so if the intrinsic curvature of radius is high, then eq.2 will be $\mu e = k\,(1/Ro^2)$.[35] In this case, R = Ro, lowering the elastic energy of the lipid monolayer, facilitating it to curl into energetically favored vesicles. This situation is only valid if no other energies compete with μe. If Ro is small then the packing stress will increase, disturbing the formation of bilayers. On the other hand, if Ro is too large it will engender a large amount of packing energy, and the bilayer is then difficult to destruct thus inhibiting release of encapsulated contents. In the case of an intermediate value of Ro, the bilayer would be stable and only could be affected by an external factor. [35]

Extrapolating from Eq.1 and Eq.2, the parameters determinative of liposome shape and stability can be predicted. To elucidate optimum conditions for liposome formation, in the work reported here, the role of (i) the length of the equilibration time after pH jump (**Δeq)**, (ii) pH jumping time (**Δjt)** which corresponds to the time interval between pHs, (iii) operation temperature (**T_o)**, and (iv) buffer type, were evaluated in terms of their effect on the critical packing shape of lipids and their spontaneous vesiculation into liposomes.

Initial method developmental work was carried out with the negatively charged phospholipid DOPG which has a very low melting temperature (T_M = - 18 °C). Once the optimal equilibrium time, pH jumping time and buffer type were evaluated, the method was demonstrated with various phospholipids specifically selected according to their surface charge and T_M values, as outlined in Table 2, and as discussed in Section 3.5.

3.2 Temperature control and Equilibrium state of the vesiculation

There are several reports of the use of a change in pH as the driving force for the formation of liposomes; however, the resulting liposomes in these reports were highly heterogeneous in size with a

mixture of GUVS, LUVs and SUVs, thus requiring further treatment to obtain liposome populations of homogenous in size.[20-26] Our studies have demonstrated that this heterogeneity in the size is principally due to a lack of temperature control and monodisperse liposome populations can be obtained under tight temperature control. In the work detailed here, temperature is used in a controlled way to adjust the curvature of the lipids in a synergetic manner with the quick jump in pH.

Moreover, not only the control of the temperature through the system but also the duration of the application of heat has an effect on the formation of vesicles. As mentioned before, in order to obtain closed packed bilayers or vesicles, the lipid packing shape should be switched from a cylindrical to a truncated cone to obtain a P value of 0.5-1, and intrinsic curvature of radius, R_o should be equal to R so as to lower the elastic energy. Increasing the applied temperature to some extent affects the fluidity of the hydrophobic tails, thus increasing the curvature, facilitating the lipid layer to curl into a liposome (see section 3.1). The first change in the lipid shape, enforced by the change in pH, is followed by a temperature provoked secondary change as the lipid aggregates curl into vesicles. Using TEM imaging, the monitoring of structural changes in the lipid aggregates over time provided powerful insight into the process of vesiculation (Figure 2). Four different equilibration times**,** 0 min, 15 min, 25 min and 45 min were studied with mixing at T_o = 45 ºC, and the **Δjt** was fixed at immediate (~1 s). Z-Potential studies were also used to characterize the stability of lipid aggregates. As can be seen in Figure 2, at **Δeq** = 0 min, at the time just after the pH jump, lipid clusters relatively homogenous in size were formed. After 15 min, the clusters show a decrease in size with an increase in surface potential (from -32 to -35 mV), whilst at **Δeq** = 25 min, monodisperse liposomes of 24.5±1.1 nm (PI=0.181) with a high surface charge of -50 mV, indicating the high colloidal stability, were observed (see Figure 2 and Table 1) .[8,15] As can be seen from Figure 2-d, when the lipid solution was left for 45 min, larger liposomes (56.7±4.7 nm (PI= 0.270)) with a sharp decrease in the surface potential (-25 mV) was observed (Table 1). Their low Z-Pot value indicates a relatively lower stability of these liposomes as compared to those formed at **Δeq** = 25 min. These results are in agreement with the data obtained from PCS measurements showing the increased mean diameter and polydispersity index 78.5±7.7 nm (PI= 0.432) of the liposomes prepared at **Δeq** = 45

min with respect to the slight increase (26.2 ±2.3 nm (PI= 0.211)) in the ones prepared at **Δeq** = 25 min after 7 months of storage at 4 °C . Although there are reports describing the increase in liposome size, with increasing duration of the hydration step for specific methods, to the best of our knowledge there is not much work explaining the change in size over time at a constant temperature. In their study, Carnerio and Santana explain the change in size by time saying that: "*The mean diameter increases with time, indicating the aggregation of lipids and a vesiculation phenomenon*".[40] However, this argument is not in agreement with our results as no sign of aggregation or fusion was observed in TEM analysis of the samples after preparation. Another study by Garcia-Manyes *et al*.[41] offered a deeper understanding of the changes in the bilayer from the perspective of molecular interactions. Basically, they stated that the temperature provokes structural changes, by softening the membrane due to several intermolecular changes, such as an increased head group area per molecule, *A*, decreased head group order and increased disorder in the hydrocarbon chains across the membrane, in a temperature range of 10 - 60 ^{o}C above T_M.[41] It is possible to hypothesise that the lipid bilayer finds the optimum chain fluidity and head group size and forms stable liposomes at around **Δeq** = 25 min. After that time period an increase in the time increases the fluidity of the tails increasing the distance between the lipid molecules resulting in less stable liposomes with larger size compared to the ones formed at **Δeq** = 25 min having a less fluid membrane (Figure 2-d).

3.3 Optimization of pH Jumping Time

The effect of the length of "jumping time", **Δjt**, was evaluated. Liposomes prepared using different **Δjt** values, immediate (~ 1 s), 0.5 min, 1 min, 15 min and 25 min, whilst T_o (45 C°) and **Δeq** (25 min) were kept constant were studied. The results were in agreement with the previous reports of Hauser *et. al* (1989), which also looked at the effect of the time interval of the pH jump.[22] An instantaneous decrease from pH 10 - 11 back to neutral pH, was observed to result in more stable liposomes. The longer the duration of the pH jump, the higher the liposome aggregation, possibly due to a lower surface potential (reduced from - 50 mV to - 37 mV) that facilitates aggregation (see Table 1). Although the degree of the

aggregation of the liposomes is acceptable for the samples prepared at 1 min of Δ**jt**, at 5 min of Δ**jt,** it is widespread and at Δ**jt** = 25 min, there are no longer vesicles but rather lipid precipitations (Figure 3).

These results can be explained by two phenomena: 1) increasing pH gradient across the membrane layer which influences the attractive/repulsive forces, affecting the stability of the bilayer,[23,42] 2) the curvature induced by an increase in the head group area/lipid molecule ratio of the lipids.[30,35] In the first phenomenon, the longer the lipids are subjected to high pH, the greater the extent of deprotonation of the head group. Thus, when the pH is reversed back to neutral, the head group charge of the lipids located in the core of the vesicles (more alkaline core) would have a higher value than the ones located on the outer layer (neutral) and this difference increases depending on the duration of the time that the lipids are left at high pH. This difference through the liposome layer may disturb the bilayer dynamics by disturbing the attractive forces keeping the lipids together in liposome form and by reducing the total surface potential of the vesicles which decreases the repulsive forces between individual liposomes which prevent them from aggregation. Some studies claim that in the case of a lipid bilayer with an alkaline inner/neutral outer core, there is lipid migration from the outer layer to inner layer depending on time and temperature.[43,44] The decreasing surface charge of the liposomes over increasing Δ**jt** is in agreement with the findings of Hope *et al*. who also reported a decrease in the surface potential (less negative membrane) of the liposomes prepared from different phospholipids, including DOPG, due to the lipid migration across the lipid bilayer (with neutral outer layer/more basic inner core). [43]

From the curvature point of view, the aggregation mechanism is similar. The higher the deprotonation of the lipid, the larger the head group area of the lipid, and the larger the intrinsic curvature of the radius, R_o, of the resulting bilayer, -in fact this is the underlying mechanism for the spontaneous formation of the liposomes due to a rapid change in pH (pH jump); however, an increased curvature difference between the inner and outer layer enlarges the packing energy which competes with the decreased elastic free energy.

As Δ**jt** increases, it promotes an increase in the packing energy of the bilayer, thus liposomes aggregate, decreasing their overall free energy.[35]

3.4 Type of Buffer solution

Liposomes are frequently employed as vesicles for the encapsulation of biological materials, such as enzymes, DNA, and drugs. Buffer type is an important factor in the encapsulation of biological molecules which require electrolyte solutions to maintain their activity. Prior to the preparation of encapsulating liposomes, one should choose the best buffer according to the needs of the encapsulated material. Here, we studied the formation of the DOPG-lyso-PPC liposomes using water and organic (HEPES and MES) and inorganic (PBS) buffer solutions of varying ionic strength (0.01 M, 0.05 M, 0.1 M, respectively), which are frequently used in encapsulating liposome preparations. Z-potential measurements, combined with TEM imaging and PCS studies, were carried out to see the relation between stability and the surface potential of the resulting forms taking into account the Derjaguin, Landau, Verwey and Overbeek (DLVO) Theory.

According to the Theory of DLVO, colloidal stability is only achieved when the repulsive forces between two particles are high enough to compete with the attractive forces (London-van der Vaals interactions):

$$V_T = V_A + V_R \qquad \text{(Eq.3)}$$

where; V_T is the interaction potential between particles, V_A is the attractive interactions and V_R is the repulsive interactions.[37] Repulsive interactions increases as a function of the Z-Pot value of two particles, which has a maxima corresponding to the highest colloidal stability with increasing ionic strength.[45]

As can clearly be seen in particle size distribution histograms in Figure 5 and TEM images in Figure 4, highly monodisperse spherical liposomes of decreasing size, 30.9 ±2.6 nm (PI=0.222) , 28.6 ±2.3 nm (PI=0.242), 24.5±1.1 nm (PI=0.181) were obtained using MES, HEPES and PBS buffers, respectively. The stability of the liposomes formed using HEPES and MES was very good, with no change in liposome size or aggregation observed over 2.5 months and a slight increase in mean diameter and PI value of vesicle population after 5 months of storage at 4 ºC (Figure 5-d and 5-f). However, the liposomes formed using PBS were notably more stable, with a smaller increase in the population size and polydispersity after at least 7 months (Figure 5-b). Z-potential studies also supported the results that the surface potential values of liposomes prepared in HEPES and MES buffers were almost the same, with a high value of ~ -42 mV, whilst the liposomes prepared using PBS have the highest Z-pot value of -50 mV (Table 1), indicative of the high colloidal stability. Liposomes prepared from different lipid formulations using either MES or PBS at same concentrations were also studied and again the liposomes prepared using PBS were more stable than those formed using MES (results not shown). This improved stability of liposomes may be attributable to the higher ionic strength of PBS compared to HEPES and MES even at the same concentration.[46] These findings are consistent with those of Claessens *et al.* (2004) who demonstrated that at a low concentration of salt in buffer, vesicle radius decreases with an increased ionic strength and the highest stability of the DOPG liposomes studied was achieved at a high salt concentration.[46] In our work, in the case of the liposomes prepared using water, the Z-Pot value was very broad, resulting in a precipitated liposome population (Figure 4-d) having a PI value of 1 indicating broad size distribution through the sample. As expected from the DLVO theory, the prepared liposomal population of unequal Z-Pot tended to aggregate due to an insufficient amount of repulsive forces over attractive forces in the absence of salt. In conclusion, the size and stability of liposomes prepared using the new method reported here are mainly related to the ionic strength of the buffer and the method works effectively in both organic and inorganic buffers.

3.5 Lipid type: T_M Value and Head Group Charge

As previously stated, it is not only the lipid packing shape but also the properties of the lipids, such as melting temperature, overall head group charge and degree of saturation, significantly affect the shape and mechanical properties of the formed liposomes.[30] Moreover, these physiochemical properties of the lipids are also important for the encapsulated material-liposome and liposome-target interactions which are essential properties of encapsulating liposomes for specific applications, such as drug delivery or gene therapy. [47-49] Therefore, here we studied several phospholipids in order to demonstrate the implementation of the method to a wide range of lipid types and also to provide a deeper understanding of the underlying mechanisms of the developed method. Lipids of different properties, negatively charged, 1,2-Dioleoyl-*sn*-Glycero-3-[Phospho-*rac*-(1-glycerol)] (DOPG) and 1,2-Dipalmitoyl-*sn*-Glycero-3-[Phospho-*rac*-(1-glycerol)] (DPPG), positively charged, 1,2-Dioleoyl-3-Trimethylammonium-Propane (DOTAP), and zwitterionic, 1,2-Dioleoyl-*sn*-Glycero-3-Phosphocholine (DOPC) and 1,2-Dipalmitoyl-*sn*-Glycero-3-Phosphocholine (DPPC), phospholipids, which as well as having differently charged head groups, also represent a wide range of T_M values (-20 to + 41 ºC), were studied. Detailed properties of the phospholipids are outlined in Table 2.

As previously mentioned, the T_M determines the phase behavior of lipids, and thus to probe the influence of lipid T_M, we prepared liposomes from lipids of different T_M, at three different operating temperatures (25 ºC, 45 ºC and 65 ºC).

Photon correlation spectroscopy studies showed that, as also can be clearly seen TEM images presented in Figure 6 b-c, the size of the liposomes prepared using negatively charged DOPG (T_M = -18 ºC) increased from 24.5±1.1 nm (PI=1.81) to 52.6±3.2 nm (PI=0.242), with an increase in the operation temperature (from 45 ºC to 65 ºC). However, in the cases of another negatively charged phospholipid, DPPG (T_M = 41 ºC) as well as the positively charged DOTAP (T_M = 0 ºC), increasing temperature only lead to a very small increase in liposome size (Figure 6). This sharp increase in the size of the DOPG

liposomes at temperatures highly above its T_M is possibly due to the lipid phase transition to a liquid-crystalline meso-phase where the lipids are more liquid [30] and the bilayer curvature is less competent against increased hydrocarbon-packing energy. In their study of different types of egg yolk lecithins with changing degree of saturations, Nii *et al.*, also reports increasing liposome size at increasing operation temperatures,[50] stating that in the case of lipids with lower degrees of saturation, corresponding to lower main-transition temperatures, T_M,[51] the increase in size becomes more significant than that of lipids with higher T_M.[50]

However, in the case of DPPG, liposomes are observed to be formed even at a temperature (25 ºC) below its T_M (Figure 6-d), which may be due to the removal of hydrocarbon-packing energy, resulting in the formation of curved structures at relatively low temperatures, by virtue of the fact that there is no other energy to compete with the curvature.[35] In a previous study, Träuble and Eibl [52] suggested that the phenomena could be due to the increased charge concentration of lipid's head group, which increases the T_M value of the lipid due to an expected change in the electrostatic free energy of the charged lipid bilayers. Hence, thanks to the head group properties of DPPG, its curvature appears to be so high following the pH jump, that it can easily overcome the packing stress caused by the hydrocarbon tails, and can form liposomes below its particular T_M value.

Concerning the behavior of zwitterionic lipids, DPPC and DOPC, the results were very different in comparison to the charged lipids. As can be seen from Figure 6-j, DOPC with T_M= - 20 ºC formed 20.2±1.4 nm (PI= 0.263) sized liposomes at just 25 ºC and nonlamellar sponge like structures at 45 ºC and 65 ºC (results not shown). Barauskas *et al*, who also obtained similar structures using a particular lipid combination of diglycerol monoolate (DGMO)/glycerol diolate (GDO)/ P80/ water, reports that in particular conditions, a decreased curvature of the lipids (e.g. heat treatment) can force the lipids to form nonlamellar mesophase structures (Sponge phase (L_3) is one of those internal mesophases).[53,54] Moreover,

in the case of DPPC (T_M = 41 ºC) and DPPG (T_M = 41 ºC), we observed the same counter-relationship as the one between DOPG and DOPC. Having the same T_M value as the negatively charged DPPG, the zwitterionic DPPC formed liposomes of 69±6.7 nm (PI= 0.281) only at 65 ºC (see Figure 6-k). At temperatures below this, it forms cubic (25 ºC) and hexagonal (45 ºC) lipid structures (results not shown) as it undergoes an insufficient curvature for the bilayer to curl into liposomes. Considering the phase theory outlined above, it is not surprising that DOPC and DPPC behave in an extremely different manner to their negative counterparts DOPG and DPPG, despite the fact that they have almost the same T_M value.

In summary, there is a strong evidence of multi-collaborative synergistic interactions of pH change, lipid type and temperature on the phase behavior of the lipids, and one can carefully tune and control the size and shape of the liposomes by taking into consideration the operation temperature and physicochemical properties of the lipids used. Although, the effect of **Δjt** was found to be same for all types of the lipids studied, one may need to re-optimize the equilibrium times for different liposome formulations of other lipid types, especially, zwitterionic lipids. Furthermore, the results indicate that as a new method, curvature tuned liposome preparation method could provide flexibility in the design of liposome-based carrier systems of different phospholipid types which is important for the immobilized/encapsulated material-lipid interaction as well as being important for the control of delivery route of the liposomes used for drug delivery systems.

5 CONCLUSIONS

A new ultra-rapid method for the preparation of liposomes and an explanation of the physical phenomena involved is reported. The developed method does not require the use of organic solvents and is completed in less than 1 hour. The method produces monodisperse liposomes of controllable size, using both charged and neutral lipids without any pre/post preparative steps. The synergistic effect of several factors, such as pH change, operation temperature, time intervals of the change in the factors or duration of them, buffer type, and lipid properties, on the bilayer curvature was investigated and formed liposomes

were analyzed using Transmission electron microscope imaging, photon correlation spectroscopy and zeta-potential measurements. The findings using different lipid types enhanced our understanding of the underlying mechanism of spontaneous vesiculation phenomenon, and allow us to predict the optimal conditions for curvature tuning of the lipid bilayer to form stable liposomes. We also demonstrated the possibility to use the method for preparation of liposomes encapsulating bioactive molecules since these liposomes were observed to be completely stable, with no evidence of leaching or aggregation, for at least seven-months of storage depending on preparation conditions. Further work will focus on the encapsulation capacities of these liposomes for the implementation of the method in applications such as drug/gene delivery, cosmetics and biosensor technologies.

ACKNOWLEDGEMENTS

This work was supported by the Commission of the European Communities specific RTD program, Smart Integrated Biodiagnostic Systems for Healthcare, SmartHEALTH, FP6-2004-IST-NMP-2-016817. We acknowledge the support from the DINAMIC Applied Biotechnology Innovation Center of Universitat Rovira i Virgili (URV) and the FI pre-doctoral scholarship of Generalitat de Catalunya. We would like to thank Esther Aules, and the technicians of Servei de Recursos Científics of URV, especially Mercè Moncusí Mercadé, for their assistance.

REFERENCES

(1) Gupta, R.B., EDs.; *Nanoparticle Technology for Drug Delivery;* Informa Health Care: USA, **2006**.

(2) Jesorka, A.; Orwar, O. The Annual Review of Analytical Chemistry **2008**, *27*, 1-32.

(3) Sharma, A.; Sharma, U. S. International Journal of Pharmaceutics **1997**, *154*, 123-140.

(4) Lasic, D.D. *Tibtech* **1998***, 16*, 307-321

(5) Crommelin, D.J.; Schreier, H., Liposomes In: Kreuter, J. EDs.; *Colloidal Drug Delivery Systems;* Marcel Dekker Inc.: New York, **1994**, Vol. *66*, 73–190.

(6) Uhumwangho, M.U.; Okor, R. S. *JMBR* **2005***, 4(1)*, 9-21.

(7) Liu, G.; Lin, Y. *Talanta* **2007***, 74*, 308-317.

(8) Rongen, H.A.H.; Bult, A.; van Bennekom, W.P. *J. Immunol Methods* **1997***, 204*, 105-133.

(9) Harasym, T.O.; Bally, M.B.; Tardi, P. *Advanced Drug Delivery Reviews* **1998***, 32*, 99-118.

(10) Nagayasu, A.; Uchiyama, K.; Kiwada, H. *Advanced Drug Delivery Reviews* **1999***, 40*, 75-87.

(11) Poznansky, J.M.; Juliano, L.R. *Pharmacological Reviews* **1984***, 36*, 277.

(12) Patil, S.D; Rhodes, D.G.; Burgess, D.J. *AAPS J. 2004;* **2004***, 6(4)*.

(13) Mamot, C.; Drummond, D.C.; Hong, K.; Kirpotin, D.B.; Park, J.W. *Drug Resistance Updates* **2003***, 6*, 271-279.

(14) Maestrelli, F.; González-Rodríguez, M.L.; Rabasco, A.M.; Mura, P. *International Journal of Pharmaceutics* **2006***, 312*, 53-60.

(15) Banerjee, R. *J. Biomaterials Applications* **2001***, 16*, 3-21.

(16) Bangham, A.D.; Standish, M.M.; Watkins, J.C. *J. Molecular Biology* **1965***, 13*, 238-252

(17) Lapinski, M.M.; Castro-Forero, A.; Greiner, A J.; Ofoli, R.Y.; Blanchard, G.J. *Langmuir* **2007***, 23*, 11677-11683.

(18) Hauser, H.; Gains, *Proc. Natl. Acad. Sci. USA* **1982***, 79*, 1683-1687.

(19) Gains, N.; Hauser, H. *Biochimica et Biophysica Acta (BBA) - Biomembranes* **1983***, 731*, 31-39.

(20) Hauser, H. *Biochimica et Biophysica Acta (BBA) - Biomembranes* **1984***, 772*, 37-50.

(21) Hauser, H.; Gains, N.; Eibl, H.-J.; Müller, M.; Wehrli, E. *Biochemistry* **1986***, 25*, 2156-2134.

(22) Hauser, H.. *Proc. Natl. Acad. Sci. USA* **1989***, 86*, 5351-5355.

(23) Hauser, H.; Mantsch, H.H.; Casal, H. L. *Biochemistry* **1990***, 29*, 2321-2329.

(24) Aurora, T.S.; Li, W.; Cummins, H.Z.; Haines, T.H. *Biochimica et Biophysica Acta (BBA) - Biomembranes* **1985***, 820*, 250-258.

(25) Ertel, A.; Marangoni, A.G.; Marsh, J.; Hallett, F.R.; Wood, J.M. *Biophysical J.* **1993***, 64*, 426-434.

(26) Mortazavi, S.M.; Mohammadabadi, M.R.; Khosravi-Darani, K.; Mozafari, M.R. *Journal of Biotechnology* **2007***, 129*, 604-613.

(27) Mozafari, M. R. *Cell Mol Biol Lett.* **2005***, 10*, 711-719.

(28) Mozafari, M. R.; Reed, C. J.; Rostron, C.; Kocum, C.; Piskin, E. *Cell Mol Biol Lett.* **2002***, 7*, 243-244.

(29) Oteka, K.; Shimomura, T.; Goto, T.; Imura, T.; Furuya, T.; Yoda, S.; Takebayashi, Y.; Sakai, H.; Abe, M. *Langmuir* **2006***, 22*, 2543-2550.

(30) Mouritsen, O.G., EDs; In *Life-As a matter of Fat (The Emerging Science of Lipidomics);* Springer: Germany*, **2005***.

(31) Nieh, M.-P.; Harroun, T.A.; Raghunathan, V.A.; Glinka, C.J.; Katsaras, J. *Biophysical J.* **2004***, 86(4)*, 2615-2629.

(32) Nieh, M.-P.; Raghunathan, V.A.; Kline, S.R.; Harroun, T.A.; Huang, C.-Y.; Pencer, J.; Katsaras, J. *Langmuir* **2005***, 21 (15)*, 6656-6661.

(33) Šegota, S.; Težak, D. *Advances in Colloid and Interface Science* **2006***, 121*, 51-75.

(34) Yue, B.; Huang, C.-Y.; Nieh, M.-P.; Glinka, C.J.; Katsaras, J. *J. Physical Chemistry* **2005***, 109*, 609-616.

(35) Gruner, S.M. *Proc. Natl. Acad. Sci. USA* **1985**, 3665-3669.

(36) Lasic, D.D.; Joannic, R.; Keller, B.C.; Frederik, P.M.; Auvra, L. *Advances in Colloidal and Interface Science* **2001***, 89-90*, 337-349.

(37) Sabín, J.; Prieto, G.; Ruso, J. M.; Álvarez R.-H.; Sarmiento F. *Eur. Phys. J. E* **2006**, *20*, 401-408.

(38) Lasic, D.D. *Biochem. J.* **1988***, 256*, 1-11.

(39) Needham, D.; Dewhirst, M.W. *Advanced Drug Delivery Reviews* **2001***, 53*, 285-305.

(40) Carneiro, A.L.; Santana, M.H.A. *Prog. Colloid Polym. Sci.* **2004***, 128*, 273-277.

(41) Garcia-Manyes, S.; Oncins, G.; Sanz, F. *J. Biophysical* **2005***, 89*, 4261-4274.

(42) Phayre, A. N., Vanegas Farfano, H. M., and Hayes, M. A. *Langmuir* **2002***, 18*, 6499-6503.

(43) Hope, M.J.; Redelmeier, T.E.; Wong, K.F.; Rodrigueza, W.; Cullis, P.R. *Biochemistry* **1989***, 28 (10)*, 4181-4187.

(44) Eastman, S.J.; Hope, M.J.; Cullis, P. R. *Biochemistry* **1991**, *30*, 1740-1745.

(45) Alonso, J.M.; Llácer, C.; Vila, A.O.; Figueruelo, J.E., Molina, F.J. *Colloids and Surfaces* **1994**, *95*, 11-14

(46) Claessens, M. M.; van Oort, B.F.; Leermakers, F.A.; Hoekstra, F.A.; Cohen Stuart, M.A. *Biophysical J.* **2004***, 87*, 3882-3893.

(47) Dabbas, S.; Kaushik, R.R.; Dandamudi, S.; Kuesters, G.M.; Campbell R.B. *Endothelium* **2008,** *15*, 189 – 201.

(48) Carrozino, J.M.; Khaledi, G.M. *Pharmaceutical Research* **2004***, 21 (12)*, 2327-2334.

(49) Rädler, J. O., Koltover, I., Jamieson, A., Salditt, T. and Safinya, C. R. *Langmuir* **1998**, 14, 4272.

(50) Nii, T.; Takamura, A.; Mohri, K.; Ishii, F. *Colloids and Surfaces B: Biointerfaces* **2002**, *27*, 323-332.

(51) Taylor, K.M.G.; Morris, R.M. *Thermochimica Acta* **1995**, *248*, 289-301.

(52) Träuble, H.; Eibl, H. *Proc. Nat. Acad. Sci. USA* **1974***, 71 (1)*, 214-219.

(53) Barauskas, J.; Johnsson, M.; Joabsson, F.; Tiberg, F. *Langmuir* **2005***, 21*, 2569-2577.

(54) Barauskas, J.; Johnsson, M.; Tiberg, F. *Nano Letters* **2005***, 5 (8)*, 1615-1619.

FIGURE CAPTIONS

Figure 1. Shematic representation of packing parameter and corresponding structure of lipid aggregate. (Modified from Ref 1).

Figure 2. TEM images of lipid organization of DOPG: lyso-PPC (88:12 mol/mol) lipid mixture at changing equilibrium time, Δ**eq**, of a) just after pH jump b) 15 min, c) 25 min, and d) 45 min. Δ**jt** = immediate (~ 1 s), T_o=45 ^{o}C , PBS buffer (pH = 7.4). Scale bar = 250 nm

Figure 3. Structural representation of the lipid aggregates formed from DOPG: lyso-PPC (88:12 mol/mol) with jumping times, Δ**jt** of a) immediate (~ 1 s), b) 0.5 min, c) 1 min, d) 5 min and e) 25 min. Δ**eq** = 25 min, T_o = 45ºC , PBS buffer (pH = 7.4). Scale bar = 50 nm

Figure 4. TEM images of DOPG: lyso-PPC (88:12 mol/mol) liposomes prepared using different aqueous solutions; a) PBS, b) HEPES, c) MES and d) Water. Δ**jt =** Immediate (~ 1 s), Δ**eq** = 25 min, T_o= 45 ºC. Scale bar = 50 nm

Figure 5. Particle size distribution histograms of DOPG: lyso-PPC (88:12 mol/mol) liposomes, prepared using different aqueous solutions as a function of storage time; (a) PBS, 1st day, (b) PBS, after 7 months of storage at 4 ºC, (c) HEPES, 1st day, (d) HEPES, after 5 months of storage at 4 ºC, (e) MES, 1st day, (f) MES, after 5 months of storage at 4 ºC, Δ**jt =** Immediate (~ 1 s), Δ**eq** = 25 min, T_o= 45 ºC. D is the mean diameter of the liposomes ± Standart deviation (SDV) calculated from the mean of the data of a series of experiments (n ≥ 3) carried out using the same parameters

Figure 6. Liposomes formed from different lipids at changing operation Temperatures, T_o, using Vesiculation Method. : (a), (b), (c) DOPG: lyso-PPC ((88:12 mol/mol)) liposomes prepared at 25 ºC, 45 ºC, 65 ºC, respectively, (d), (e), (f) DPPG: lyso-PPC (88:12 mol/mol) liposomes prepared at 25 ºC, 45 ºC, 65 ºC, respectively, (g), (h), (i) DOTAP: lyso-PPC (88:12 mol/mol) liposomes prepared at 25 ºC, 45 ºC, 65 ºC, respectively, (j) DOPC: lyso-PPC (88:12 mol/mol)) liposomes prepared at 25 ºC, (k) DPPC:

lyso-PPC ((88:12 mol/mol) liposomes prepared at 65 ºC. Δ**jt** = Immediate (~ 1 s), Δ**eq** = 25 min, PBS buffer (pH = 7.4). Scale bar = 100 nm

TABLES

Table 1. List of the operation parameters studied and corresponding Z-Potential values, mean diameter and polydispersity index (PI) of DOPG: lyso-PPC (88:12 mol/mol) liposomes. Δ**jt** is the interval of pH jump and Δ**eq** is the duration of equilibrium step at a certain temperature. * Unequal Z-Pot values of three repetitions. ** A particle population is accepted as monodisperse when the polydispersity index, PI, is in the range of 0-0.5. A value higher than this shows heterogeneous size distribution.

Table 2. Properties of the phospholipids evaluated for preparation of liposomes using developed method.

Critical Packing Parameter ($P=v/a.l$)	Critical Packing Shape	Structure Formed
< 1/3		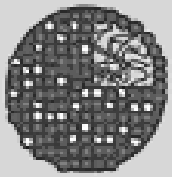
1/3-1/2		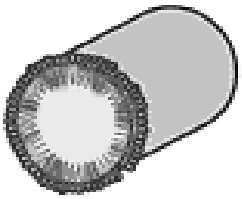
1/2 – 1		
~1	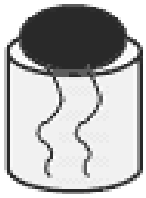	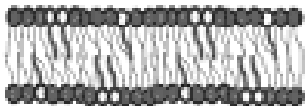
>1		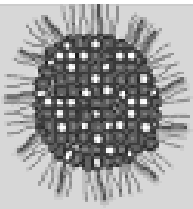

Figure 1

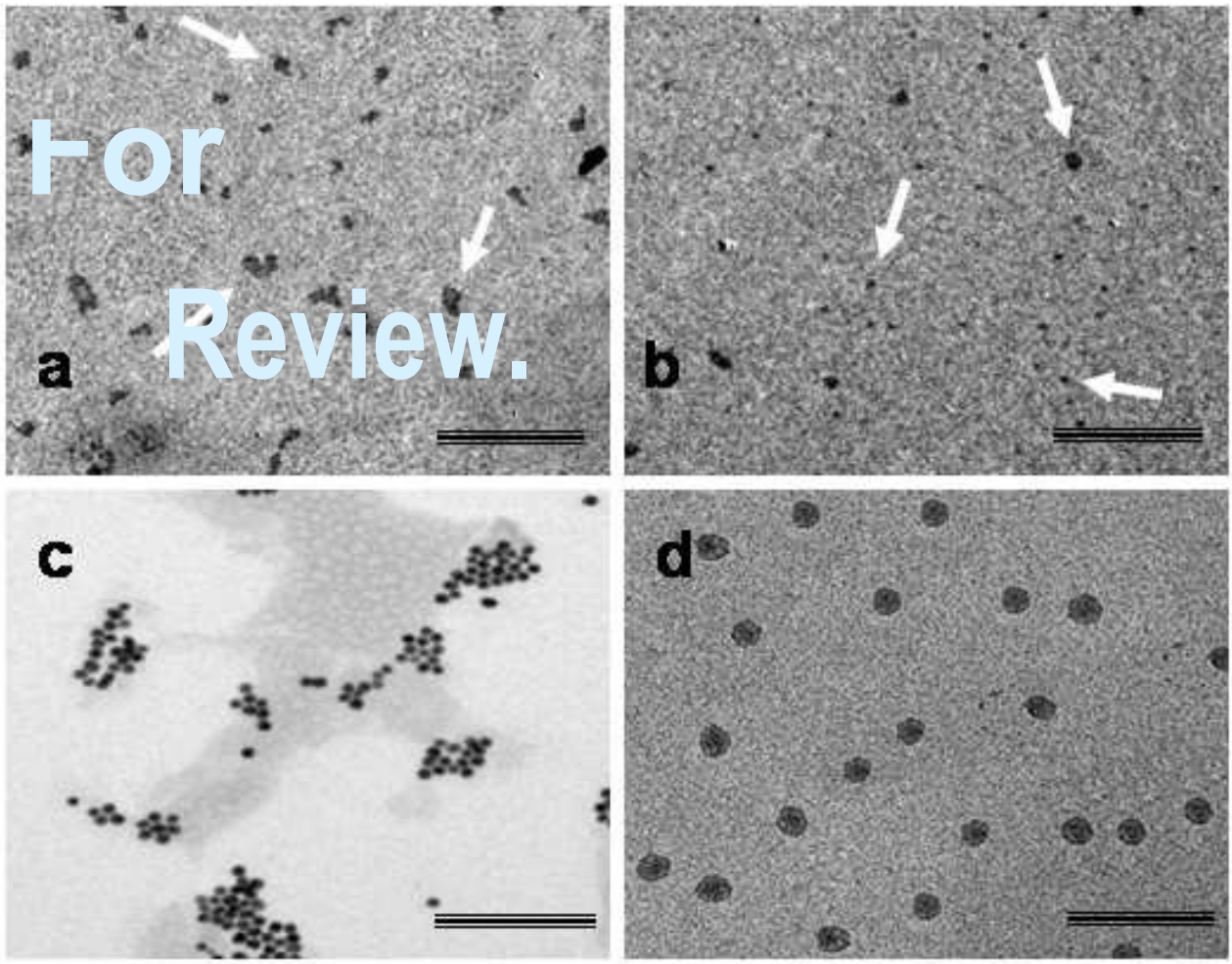

Figure 2

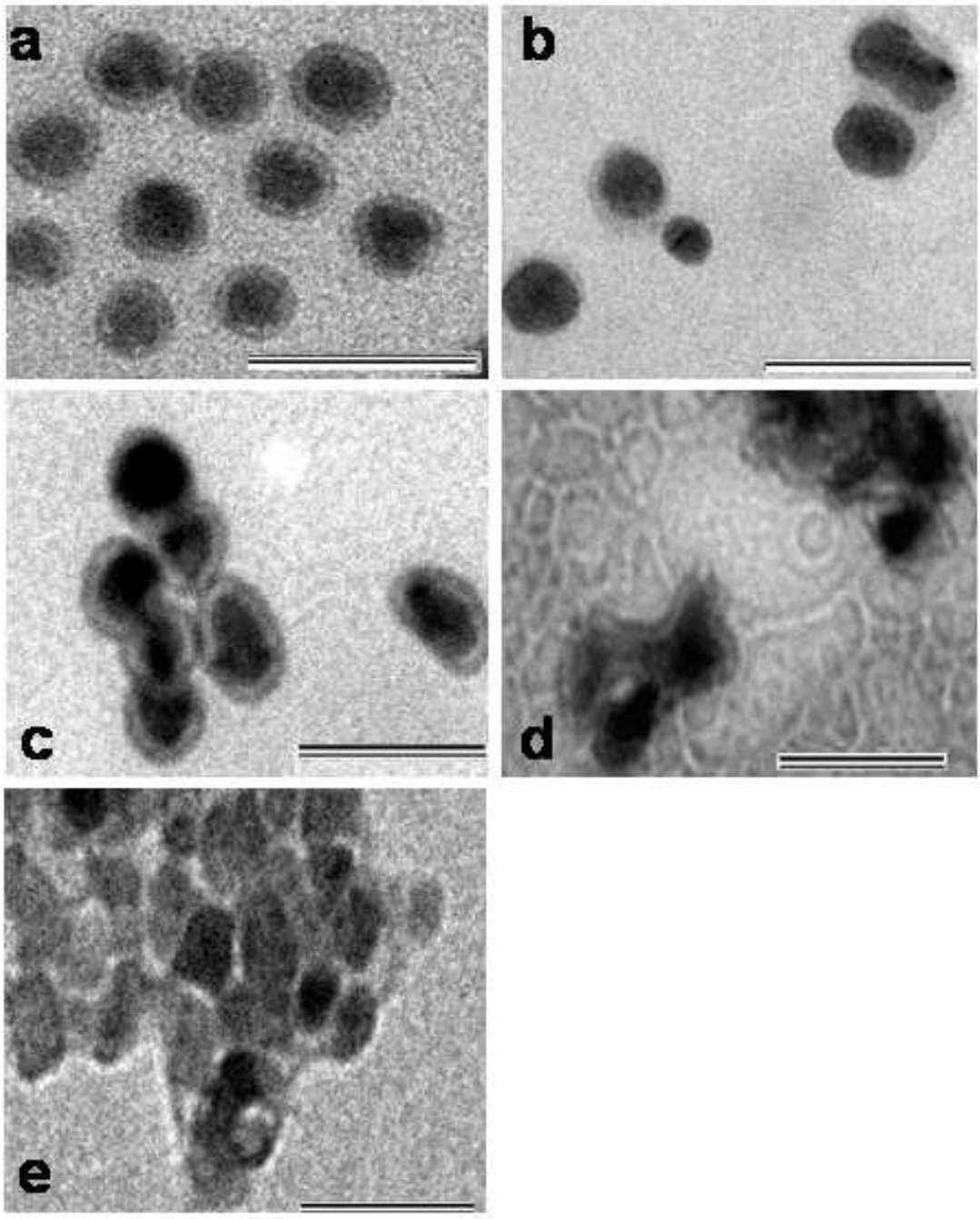

Figure 3

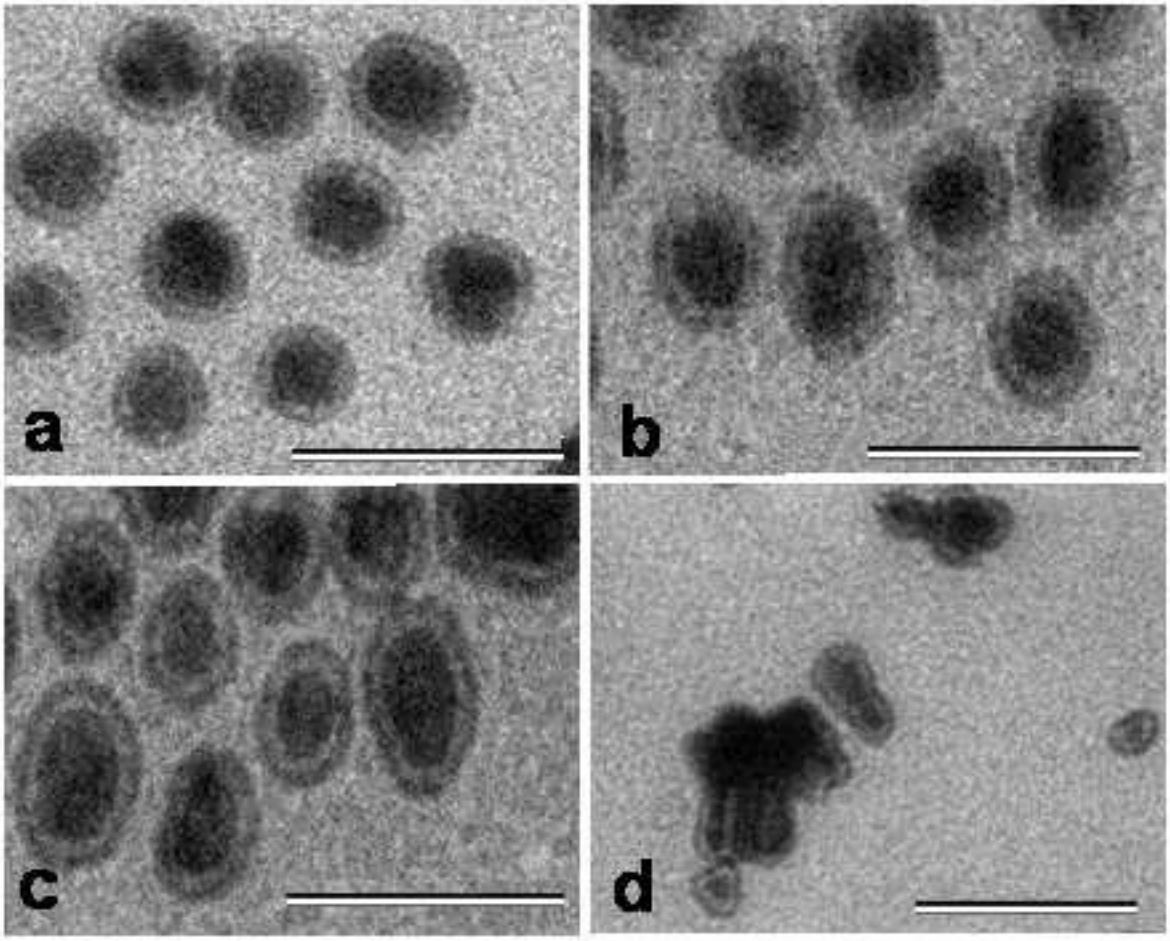

Figure 4

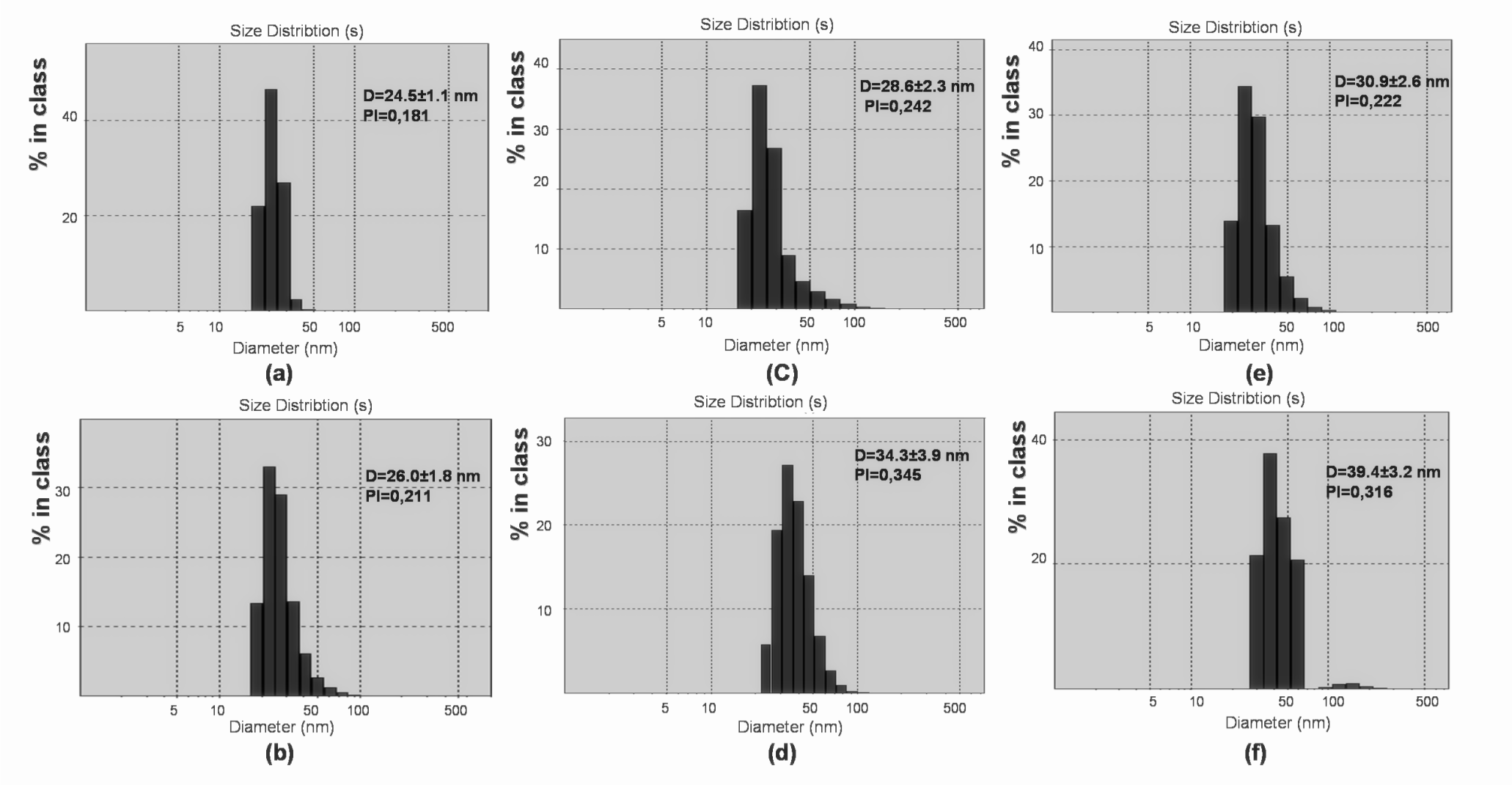
Size Distribtion (s)
% in class
D=24.5±1.1 nm
PI=0,181
Diameter (nm)
(a)
Size Distribtion (s)
% in class
D=28.6±2.3 nm
PI=0,242
Diameter (nm)
(C)
Size Distribtion (s)
% in class
D=30.9±2.6 nm
PI=0,222
Diameter (nm)
(e)
Size Distribtion (s)
% in class
D=26.0±1.8 nm
PI=0,211
Diameter (nm)
(b)
Size Distribtion (s)
% in class
D=34.3±3.9 nm
PI=0,345
Diameter (nm)
(d)
Size Distribtion (s)
% in class
D=39.4±3.2 nm
PI=0,316
Diameter (nm)
(f)

Figure 5

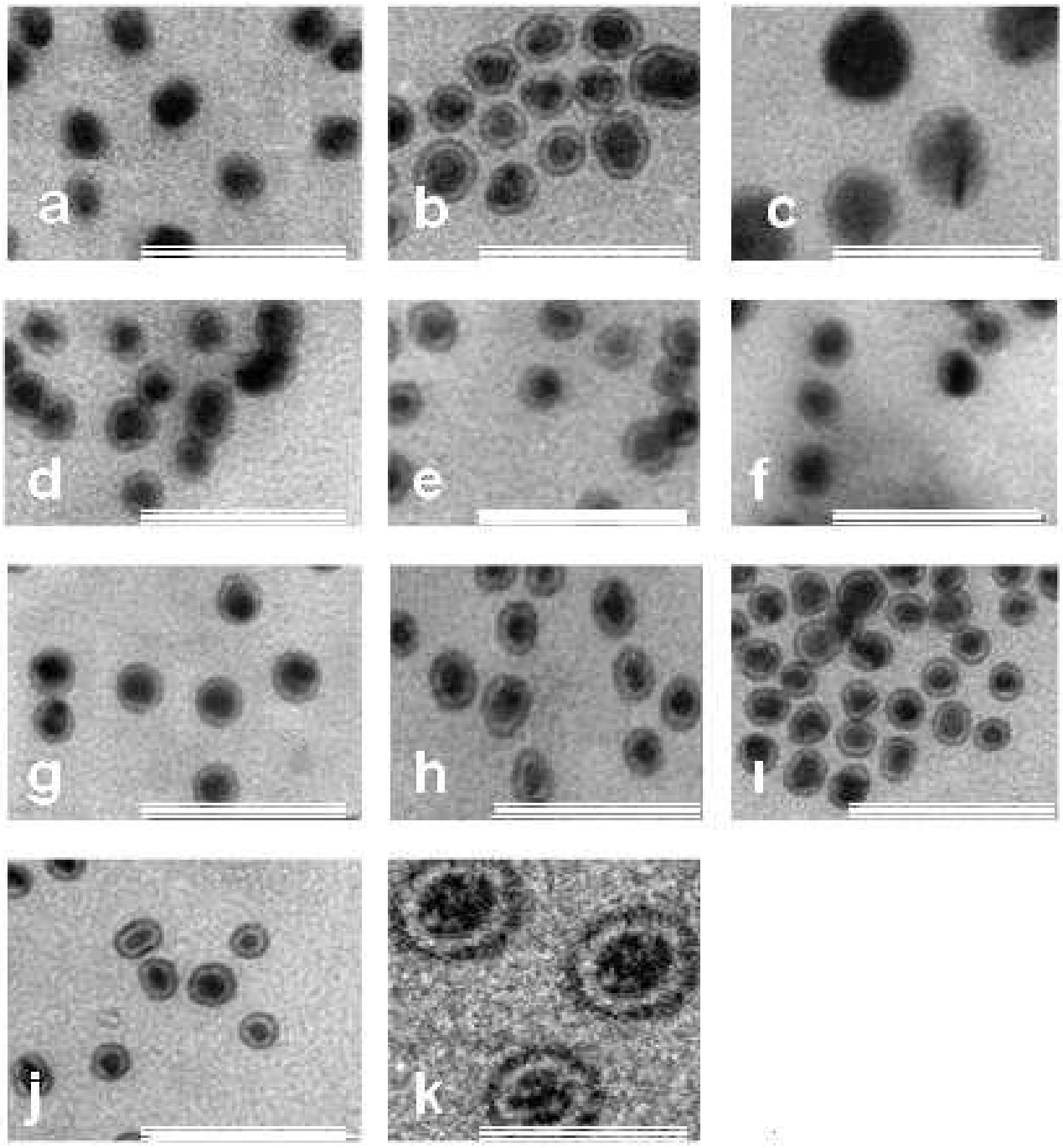

Figure 6

Operation Temperature(T_o) (°C)	Δ_{jt} (min)	Δ_{eq}(min)	Buffer Type	Mean Diameter nm±SDV (n=3)	PI Value **	Z-Potential mV ± SDV (n=3)
45	Immediate (~1s)	0	PBS	–	1	**-34.6 ±4.9**
45	Immediate (~1s)	15	PBS	–	1	**-35.4 ±6.8**
45	Immediate (~1s)	25	PBS	24.5±1.1	0.181	**-50.1±3.3**
45	Immediate (~1s)	45	PBS	56.7±4.7	0.249	**-24.9 ±4.9**
45	0.5	25	PBS	–	–	**-47.1 ±3.6**
45	1	25	PBS	–	–	**-45.2 ±4.1**
45	5	25	PBS	–	–	**-36.4 ±3.9**
45	25	25	PBS	–	–	**-37.2 ±13.8**
45	Immediate (~1s)	25	WATER	–	1	**-56.2 ±106.0 ***
45	Immediate (~1s)	25	HEPES	28.6 ±2.3	0.240	**-41.1 ±4.6**
45	Immediate (~1s)	25	MES	30.9 ±2.6	0.222	**-40.8 ±4.9**
25	Immediate (~1s)	25	PBS	22.4±1.0	0.200	**-47.5 ±3.8**
65	Immediate (~1s)	25	PBS	52.6±3.2	0.242	**-43.6 ±4.9**

Table 1

Lipid name	Chemical Structure	Degree of Saturation	Surface charge	T_M(°C)
1,2-Dioleoyl-*sn*-Glycero-3-[Phospho-*rac*-(1-glycerol)] (Sodium Salt) (DOPG)	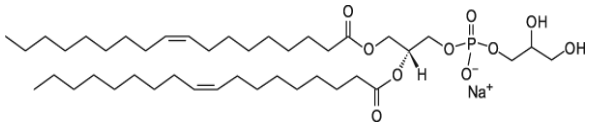	18:1	Negative	**-18**
1,2-Dipalmitoyl-*sn*-Glycero-3-[Phospho-*rac*-(1-glycerol)] (Sodium Salt) (DPPG)	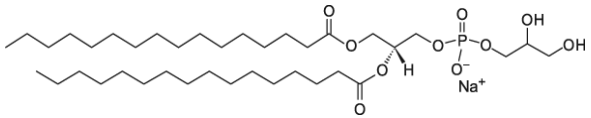	16:0	Negative	**41**
1,2-Dioleoyl-3-Trimethylammonium-Propane (Chloride Salt) (DOTAP)	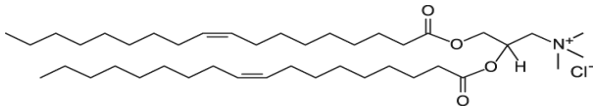	18:1	Positive	**0**
1,2-Dioleoyl-*sn*-Glycero-3-Phosphocholine (DOPC)	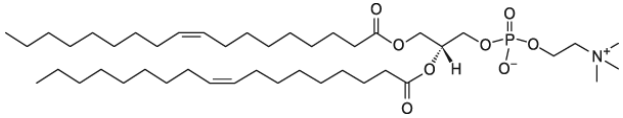	18:1	Zwitterion	**-20**
1,2-Dipalmitoyl-*sn*-Glycero-3-Phosphocholine (DPPC)	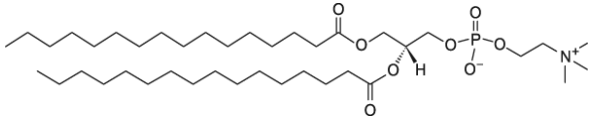	16:0	Zwitterion	**41**

Table2

TABLES OF CONTENT GRAPHIC